Design and Fabrication of 1x2 Multimode Interference Coupler Using Photosensitive Permanent Material for Wavelength Division Demultiplexing

Abdullahi Usman[1], Ravivudh Khun-in[2*], Apichai Bhatranand[2], Yuttapong Jiraraksopakun[2], Salinee Choowitsakunlert[2], Thorin Theeradejvanichkul[2], and Hideki Yokoi[3]

[1]Department of Physics with Electronics, Federal University Birnin Kebbi, P.M.B 1157, Nigeria
[2]Department of Electronic and Telecommunication Engineering, Faculty of Engineering, King Mongkut's University of Technology Thonburi, Bangkok 10140, Thailand
[3]Department of Electronic Engineering, College of Engineering, Shibaura Institute of Technology, Tokyo 135-8548, Japan

Abstract: This report presents a 1x2 multimode interference coupler using photosensitive permanent material for wavelength division demultiplexing (WDM). The multimode interference (MMI) for multiplexer (MUX) and/or demultiplexer (DEMUX) architectures used different coupling lengths at long beat lengths for individual signal propagation. The MMI design was proposed with a short beat length and a single coupling length of two signals. The proposed MMI of a 1x2 coupler was simulated with the beam propagation method (BPM) using silicon dioxide (SiO_2) and photosensitive permanent material "TMMR-S2000" as the cladding and core with the refractive indices of 1.45 and 1.57, respectively. The two light signals with 1310 nm and 1550 nm wavelengths were propagated through the 2.8 m wide input waveguide section, with the coupling length and width of 510 μm and 6.7 μm, respectively. The MMI was later fabricated using conventional photolithography with the help of hard baking. The simulation results showed that a high percentage of the two signals' splitting power was realized. The performance characterization of the system was determined in terms of the insertion loss and extinction ratio. According to the numerical simulations, the extinction ratios for 1310 nm and 1550 nm lights are 19 dB and 17 dB, respectively, and the insertion losses for these wavelengths are 0.97 dB and 0.46 dB, respectively. When comparing the simulation results of the intensity distribution with the near-field patterns of the fabricated MMI at a coupling wavelength of 1310 nm, the desired splitting results were achieved. The proposed system can be used for multiplexing, demultiplexing, and optical coupling techniques to achieve a high data bitrate while maintaining low back reflection in optical communication systems. However, at 1550 nm, the findings were unfavourable.

***Keywords*— Coupler, Fabrication, Multimode interference, Wavelength division multiplexing**

I. INTRODUCTION

Optical communication has become one of the most efficient communication networks for mobile and satellite communications, employing integrated passive components and signal transmission with lower insertion loss. The MMI coupler has been advancing with multiple applications in photonic integrated circuits [1,2], such as wavelength division multiplexing (WDM), wavelength division demultiplexing, and Mach-Zehnder interferometer with the help of splitter and combiner [3-5]. Different coupling mechanisms have been implemented, like two identical parallel waveguides with equal width, where light propagates at a closed separation apart, or a Mach-Zehnder interferometer with a Y-splitter, as reported in [6]. According to the principle of the interference coupler in [7], the input signal from one mode was transferred to the output of the other mode. Many MMI research findings have been published regarding the number of input/output signals for power handling, insertion loss, back reflection, and device performance using self-imaging [8,9]. Self-imaging is the process whereby an input signal to the homogenous multimode region produces single or multiple outputs at the propagation length.

According to [10], a 1x2 MMI coupler was realized with a non-crystalline diamond and silica-on-silicon substrate as the core and cladding, respectively, with a very small width of 2.4 mm used to eliminate the risk of the output waveguide being affected by the output ports. The MMI was simulated with various beat lengths using the BPM, and the most effective one was 50.7 microns. A promising result with a high percentage output energy and lower crosstalk was achieved, but it would be difficult to fabricate with a short waveguide

This paragraph of the first footnote will contain the date on which you submitted your paper for review.

*Corresponding author: Ravivudh Khun-in, Department of Electronic and Telecommunication Engineering, Faculty of Engineering, King Mongkut's University of Technology Thonburi, Bangkok 10140, Thailand (Email: ravivudh.khu@kmutt.ac.th)

length and narrow width. In [11,12], a 1x4 DEMUX based on the cascades of three 1x2 MMI was simulated with the BPM combined with finite different time domain (FDTD) at the wavelength of 1530, 1540, 1550, and 1560 nm, with the silicon nitride (SiN) and silicon oxide (SiO_2) as the core and cladding layers, respectively. A low back reflection with a high data bitrate was achieved, but the system was quite complex and had a cascaded connection.

The 2x2 coupler in optical waveguide filters based on multimode interference is simulated using BPM [13]. This work reports 1300- and 1550-nm light operations were reported with the silicon-germanium and silicon as the core and cladding layers, respectively. Both filters achieved a remarkable insertion of less than 0.1 dB, but different coupling lengths of 5180 and 4710 microns for the 1310 and 1550 nm were used [14]. Based on the aforementioned, the MMI couplers of both splitting and combining signals were formed at different signal coupling lengths. In this work, a 1x2 MMI coupler was proposed at a fixed coupling length of both signals through photo patternable permanent materials for structure fabrication photosensitive permanent material (TMMR-S2000) deposited on the substrate, with refractive indices of 1.57 and 1.45, respectively. The TMMR-S2000, reported in [15,16], offered low-temperature curing and negative photosensitive permanent liquid type with excellent resolution and high adhesion, allowing the production of patterns with a high aspect ratio. The TMMR-S2000 could be employed to form cavity structures and insulation layers for semiconductor integration and channels for microelectro-mechanical systems (MEMS) devices.

II. MATERIALS AND METHODS

The MMI is a single passive device comprising multiple inputs and outputs, either as a splitter or combiner. In this paper, the 1x2 MMI DEMUX consists of three segments, i.e., one input single-mode waveguide, a multimode waveguide, and two output single-mode waveguides. The single input segment is used to supply two wavelengths (1310 nm and 1550 nm), and two output segments are applied to split the two signals. The waveguide is analyzed based on the 2-D lateral and longitudinal structure, which can be obtained from the actual 3-D physical MMI [4].

2.1 Propagation Constants

According to [14], the propagation constant must satisfy the dispersion equation. The dispersion equation is given in (1).

$$K_{y_m}^{\ 2} + \beta_m^2 = K_0^2 n_1^2 \tag{1}$$

$$K_0 = \frac{2\pi}{\lambda} \tag{2}$$

$$K_{y_m} = \frac{(n+1)\pi}{W_e} \tag{3}$$

where K is the lateral wavenumber along the y_m-axis of the lateral modes m, n is the number of propagating modes. K_0 is the propagation constant, λ is the light wavelength, W_e is the effective width, and β_m is the longitudinal propagation constant. The effective width W_e of transverse magnetic (TM) mode is presented as [14].

$$W_e = W_{MMI} + \left(\frac{\lambda}{\pi}\right)\left(\frac{n_2}{n_1}\right)^{2\alpha}(n_1 - n_2)^{-\frac{1}{2}} \tag{4}$$

where W_{MMI} is the physical width and n_2 is the refractive index of the cladding. The α value can either be 0 or 1 for transverse electric field (TE) and transverse magnetic (TM) modes, respectively. The propagation constant can be achieved by inserting (2) - (4) into (1) to get.

$$\beta_m = \sqrt{K_0^2 n_1^2 \left(\frac{(n+1)\pi}{W_{MMI}}\right)^2} \tag{5}$$

By using the Taylor expansion, (5) becomes

$$\beta_m = n_1 K_o \frac{(n+1)^2 \pi\lambda}{4 n_1 W_e^2} \tag{6}$$

The propagation constant difference between the fundamental and any other modes can be presented as

$$\beta_0 - \beta_m = \frac{n(n+2)\pi\lambda}{4 n_1 W_e^2} \tag{7}$$

where β_0 is the fundamental mode propagation constant, β_m is the propagation constant of the m^{th} mode. The coupling measurement is related to the interference that depends on the propagation constant between the two fundamental modes, which are the first mode and any other mode, as presented in [14]. A 3D schematic diagram of the multimode interference coupler is depicted in Fig.1.

.

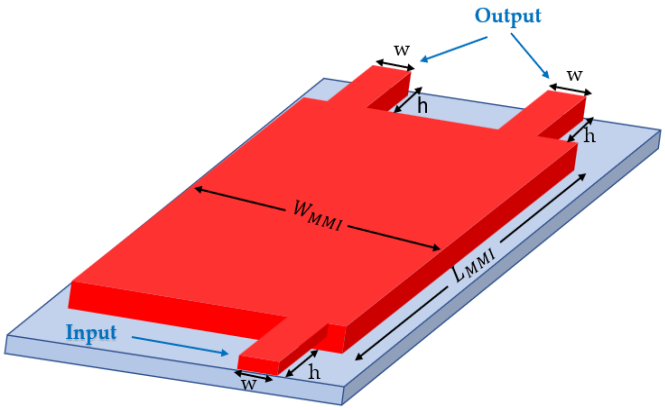

Fig. 1. Schematic diagram of multimode interference coupler.

The beat length L_π between the two modes is related to the interference among them as given in (8).

$$L_\pi = \frac{\pi}{\beta_o - \beta_m} \approx \frac{n(n+2)}{3L_\pi} \tag{8}$$

The beat length at the first mode can be written as

$$L_\pi = \frac{4n_1 w_e^2}{3\lambda_o} \tag{9}$$

In Fig. 1, W_{MMI}, L_{MMI}, are the physical width and propagation length of the MMI segment, respectively, while w and h are the width and length of both input and output waveguide segments, respectively. The signals are interfered with as they propagate through the main MMI, which creates an image related to the beat length. The power transmission between each output influences the beat length. Therefore, the most important thing is to find the appropriate length of multimode interference (L_{MMI}). The propagation constant difference can be written as

$$\beta_0 - \beta_1 = \frac{n(n+2)\pi}{3L_\pi} \tag{10}$$

The L_{MMI} can be obtained as follows,

$$L_{MMI} = \frac{P}{N} 3L_\pi \tag{11}$$

where P is an integer referring to the periodic nature of the image along the multimode waveguide and N is the number of the laser sources (i.e., N=2). These numerical values of the L_π and L_{MMI} are computed for the two wavelengths as presented in Table 1. The *2D* schematic of the signal coupling and splitting at various propagation lengths in the proposed 1x2 MMI is presented in Fig. 2. The signal power is transferred in the waveguide segment at each stage of the beat length as shown in Fig. 2. The two signals (λ_1 and λ_2) can be detected at the either output 1 or output 2. This shows that the 1550 nm signal at the beat length of 3Lπ can be detected at output 1, while the other signal of 1310 nm at the beat length of 6Lπ can be found at output 2. The relationship between the extinction ratio and insertion loss in the input and output signals can be used to characterize the MMI filter's performance. The insertion loss and extinction ratio can be determined as

$$\text{Insertion Loss} = -10\log_{10}\left(\frac{P_1}{P_i}\right) \tag{12}$$

$$\text{Extinction Ratio} = 10\log_{10}\left(\frac{P_1}{P_2}\right) \tag{13}$$

where P_i is the input power, P_1 is the desired output power and P_2 is the undesired output power.

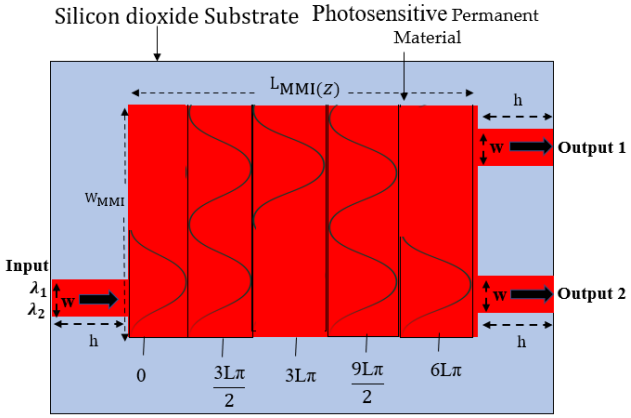

Fig. 2. Schematic of the signal coupling and splitting at various propagation lengths.

III. FABRICATION AND MEASUREMENT

The TMMR-S2000 is used for the first time to produce the MMI. According to the schematic diagram of fabrication processes depicted in Fig. 3, the MMI made up of negative photoresist (TMMR-S2000), coated by spin coater at the rotation condition of 4000 rpm in 30 seconds on 10×5 mm^2 Si glass substrate of thickness 5 mm, to form a TMMR-S2000 layer of thickness of about 10 microns. A two pre-baking is done by placing the deposited in the hot plate at 60 °C for 5 minutes and 90 °C for 5 minutes. On the other hand, the MMI mask was designed with the help of AR_CAD software with the simulation parameters to position the fabrication process in the maskless photolithography as it has been achieved in the fabrication of liquid crystal elastomers with the same technique [15]. The ultraviolet light of 75,000 mJ/cm^2 was then exposed with maskless lithography using Nano-System Solutions: model DL-1000GS/SS onto the deposited TMMR-S2000 for 20 minutes with the autofocusing of 0.04 mm [16].

A post-exposure baking was performed at 90°C for 5 minutes to develop the structure. Finally, a hard bake was performed by placing the designed mask on top of the glass substrate, which had a dimension of 10 × 5 mm^2. The waveguide was printed and then baked on a hot plate at 100 °C for 10 minutes. As the negative photoresist was used, the surface exposed to UV light was removed and left behind the unexposed one.

VI. RESULTS AND DISCUSSION

VI.I Simulation Result

The simulation of the MMI coupler was performed with TM mode using Rsoft photonic CAD software based on the BPM. The two signals with 1310 nm and 1550 nm wavelengths were introduced into the multimode waveguide through the single-mode input waveguide segment. The widths of the input and output segments were chosen to be 2.8 μm with a length of 100 nm and the width of the main waveguide (W_{MMI}) of 6.7 µm. According to the different beat length values presented in Table I, the desired (L_{MMI} could be chosen as the beat length for each signal. In the simulation, the L_{MMI} was adjusted until an optimum beat length value of 510 nm was obtained for both wavelengths of 1550 nm and 1310 nm. When looking at the intensity distribution and normalized power, it could be seen that the power was not equally divided because the principle of directional coupler was applied (10 dB). Hence, the power was divided into 10% and 90% at coupling and direct outputs. The performance of the MMI could be characterized in terms of an insertion loss and an extinction ratio. From (8) and (9), the numerical values of the insertion loss of light signals with 1310 nm and 1550 nm wavelengths were 0.97 dB and 0.46 dB, respectively. Meanwhile, the corresponding extinction ratios for 1310 nm and 1550 nm light signals were 19 dB and 17 dB, respectively. The intensity distribution of the two MMIs was depicted in Fig. 4, and the normalized power of the respective distributions was plotted using MATLAB, as illustrated in Figs 5 and 6, respectively. It is important to clarify that a short beat length denotes a brief propagation distance from the input to the output, while the coupling length refers to the transmission channel between the two signals. In this study, a single coupling length is established as the optimal propagation length that allows the generation of two signals at different outputs, with a short beat length of 510 µm.

TABLE I
BEAT LENGTH PROPAGATION VALUES

λ(nm)	L_{MMI_0}	L_{MMI_1}	L_{MMI_2}	L_{MMI_3}	L_{MMI_4}
	0	3Lπ/2	3Lπ	9/2Lπ	6Lπ
1310	0	37.72	75.45	113.17	150.9
1550	0	112.5	225.35	338.03	450.714

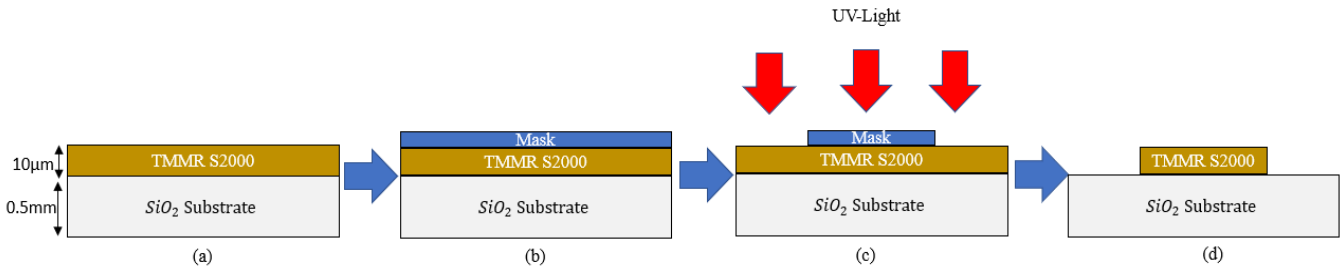

Fig. 3. The schematic diagram of the microfabrication processes: (a) TMMR S2000 is deposited on the SiO_2 substrate, (b) Desired mask is placed on top of the TMMR S2000, (c) An UV-light is exposed on the unmasked TMMR, and (d) The MMI is formed on the unexposed TMMR surface.

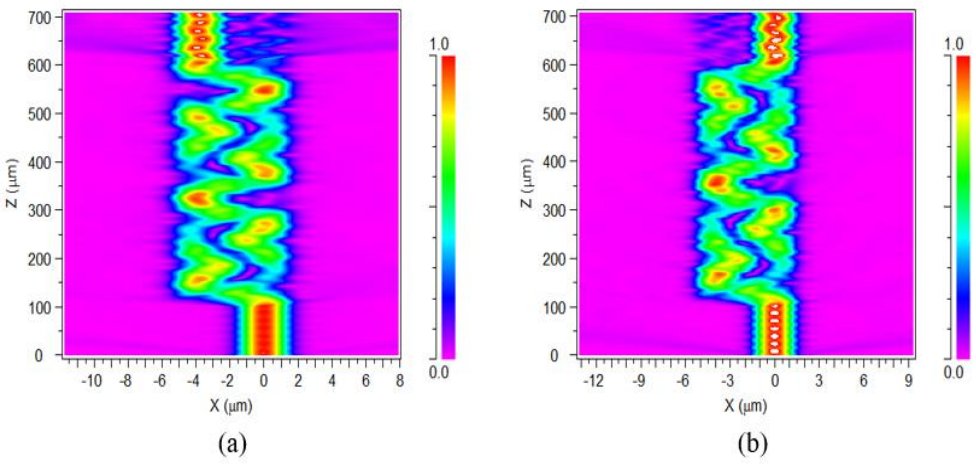

Fig. 4. Intensity distributions of the 1×2 TMMR-S2000 MMI demultiplexer: (a) λ_1 = 1550 nm (port 1), (b) λ_2 = 1310 nm (port 2).

T TABLE II
INPUT/OUTPUT POWERS INCLUDING INSERTION LOSS AND EXTINCTION RATIO

Wavelength (nm)	Input (a.u)	Port 1 Output (a.u)	Port 2 Output (a.u)	Insertion loss (dB)	Extinction Ratio (dB)
1310	9.74×10^{-1}	9.95×10^{-3}	7.79×10^{-1}	0.97	19
1550	9.72×10^{-1}	8.73×10^{-1}	1.52×10^{-2}	0.46	17

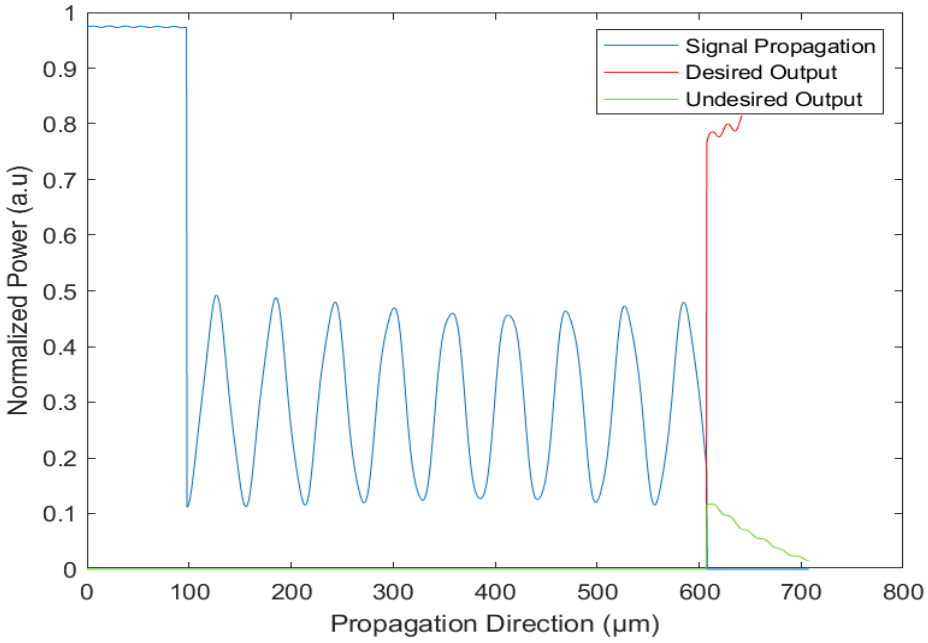

Fig. 5. Normalized power of 1550 nm light signal

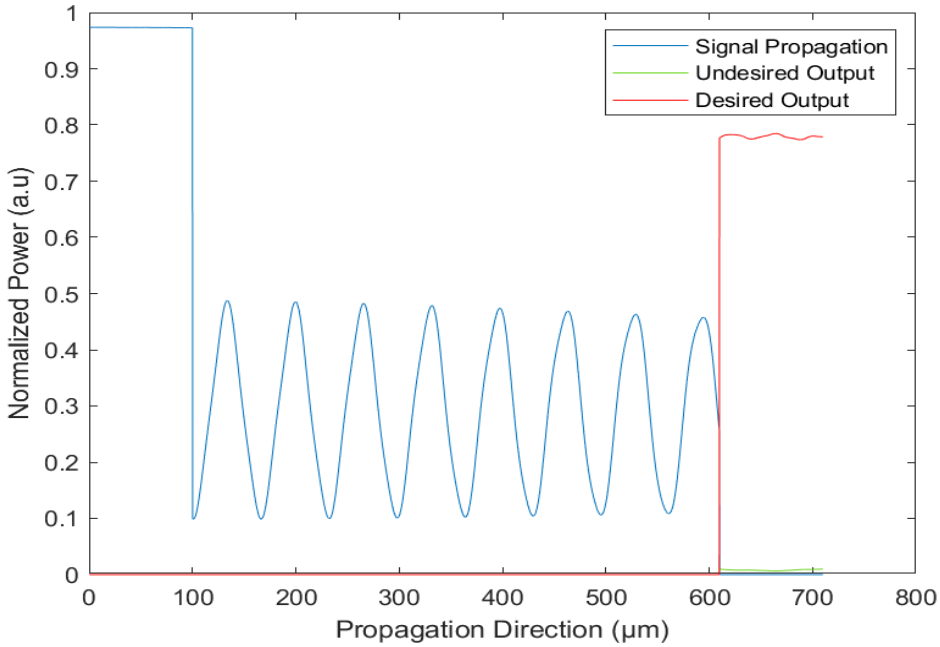

Fig. 6. Normalized power of 1310 nm light signal.

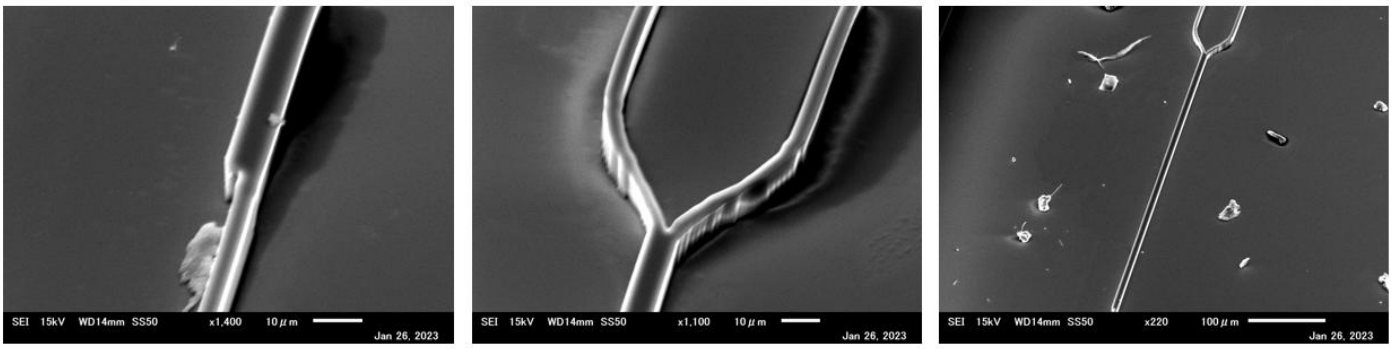

(a) (b) (c)

Fig. 7. The SEM 3D view of the MMI coupler of (a) input port (b) output port and (c) main waveguide.

A fully automated sputter coater was used to perform a vacuum sputtering with gold particles of 1nm thickness and deposit them on the MMI. The gold deposition was then inspected using a Scanning Electron Microscope (SEM) of SmartLab Rigaku Corporation model: JSM-6010LV. Thus, the input, output, and primary waveguide structures, as shown in Fig. 7, were all examined using the SEM.

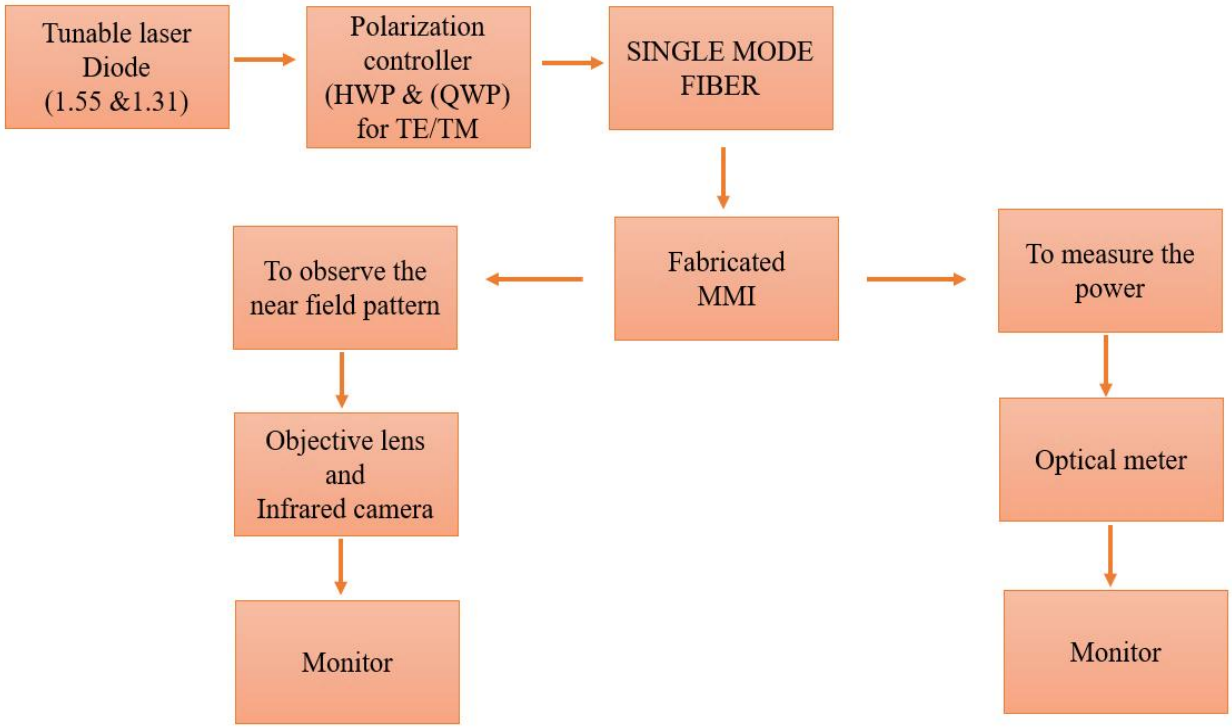

Fig. 8. Diagram of the near field pattern and optical power measurement of the fabricated waveguide.

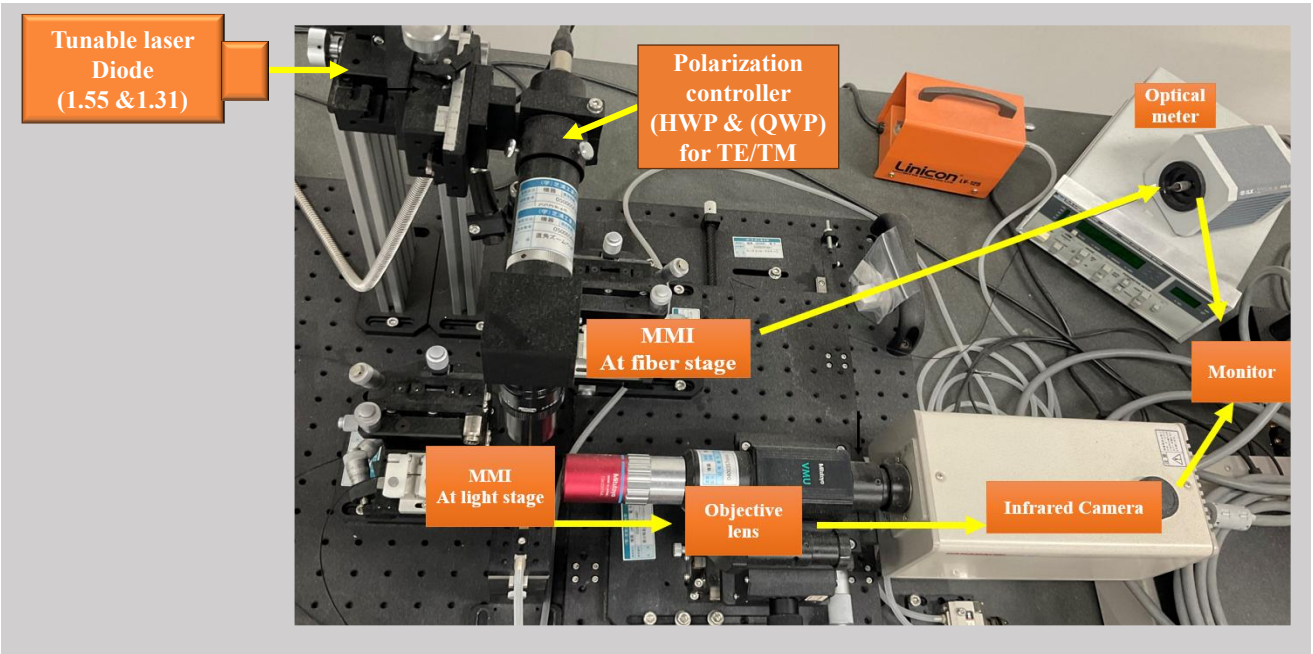

Fig. 9. Experimental setup of near-field pattern and intensity measurements.

VI.II Experimental results

According to [16], a two-channel SiN MMI coupler is simulated and divided between 1540 and 1560 nm. A single beat length is optimized as the coupling length to split the two wavelengths. A significant aspect of low back reflection is achieved. However, splitting the signal at closed wavelengths from 1530-1570 nm is very insignificant, and the simulated result was not practically implemented. It was assumed that determining the optimum beat length, which splits both wavelengths, is the only way to fabricate a single waveguide of MUX or DEMUX applications. According to the schematic diagram depicted in Fig. 8 and implemented in Fig. 9, the fabricated waveguide was placed on the setup stage to observe the near field pattern and optical splitting power separately, using butt-coupling to the single mode fiber at both input and output ports, as reported in [17]. Two light sources emitting lights with wavelengths of 1550 nm (Hewlett Packard: 8168F) and 1310nm (Ando: AQ4211LD) were used with a polarization controller (Oxide corporation) mounted with a half-wave plate (HWP) and a quarter-wave plate (QWP) to produce linearly polarized light beams. The HWP and QWP were adjusted to generate a TM mode light propagating through a single-mode fiber. The MMI was then focused through the objective lens (Mitatuyo: J24029705A) attached to the camera (Hamamatsu Photonics), allowing the near-field pattern to be shown on the screen. After that, the proposed multi-mode interferometer (MMI) was mounted on the fiber coupling stage. The optical power was measured using an optical power meter (LIGHTWAVE: FPM-8210), which was connected to a screen to display the optical intensity profile. The results are illustrated in Fig. 10. The desired near-field pattern was achieved with the 1310 nm light wave; however, an undesirable pattern was observed with the 1550 nm light signal due to low signal transmission between the two output ports.

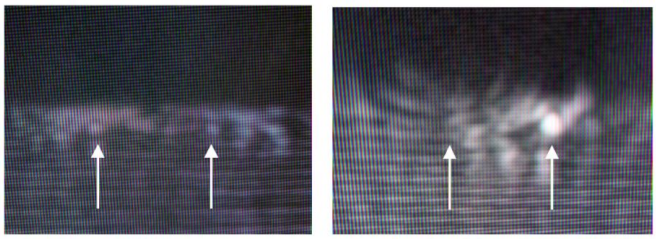

(a) (b)

Fig. 10. The MMI near field patterns of (a) 1550-nm and (b) 1310-nm light waves.

V. CONCLUSION

Two wavelengths can be self-imaged to propagate at a common coupling beat length, as reported in [16]. The notable contribution of this research is the 1x2 MMI coupler for the two wavelengths demultiplexer of 1310 nm and 1550 nm with a single coupling beat length of 510 nm for both signals, was simulated with RSoft, a BPM-based software. The proposed device was successfully fabricated using the photolithography technique using a negative photoresist (TMMR-S2000: Tokyo Ohka Kogyo or TOK). The microfabrication of the MMI mask was formed on the TMMR-S2000 layer deposited on the SiO_2 substrate. The simulation results revealed excellent performance, with insertion losses of 0.97 dB and 0.46 dB for light waves at 1310 nm and 1550 nm, respectively, and extinction ratios of 19 dB and 17 dB, respectively.

In contrast to other reports, which found that various signals were split at different beat lengths with longer propagation lengths, this proposed approach could separate signal wavelengths at a fixed and shorter beat length. The 1x2 MMI was successfully fabricated with high-temperature baking and conventional photolithography. The near-field pattern of the MMI was observed and depicted in Figs 9 and 10. By comparing the simulation result shown in Fig. 4(a) with that of the experimental near-field pattern depicted in Fig. 10(a), the undesired splitting results were obtained for a 1550 nm light wave. The desired near field pattern was only accomplished for the 1310 nm light wave, as shown by the simulation finding in Fig. 3(b) and an experiment result in Fig. 10(b). Since the optical power could hardly be detected at the wavelength of 1550 nm, the undesirable output was seen, as illustrated in Fig. 10(a). While the 1550 nm wavelength results need improvement, the proposed scheme shows promise for the 1310 nm wavelength, which is the primary wavelength for upstream transmission in FTT. This research highlights the innovative use of photosensitive permanent material for multimode interferometers or MMI. The system can be further studied in 2 x2 multimode multiplexing, where the two signals are utilized at the input, and a desired signal at the desired output is detected based on the propagation lengths computations. This technique is applicable in minimizing back reflection in optical waveguide communication systems.

References

[1] Jin-Song X, Jin-Zhong Y, Zhong-Chao F, Zhang-Tao W and Shao-Wu C 2004 *Chinese Physics Letters* 21 104

[2] Yan-Zhe, T, Ke-Miao J, Bai-Yang L, Jian-Yi Y, Xiao-Qing J, Ya-Ming W and Yue-Lin W 2004 *Chinese Physics Letters 21* 1064

[3] Mizera T, Pudiš D, Kuzma A, Gašo P, Miček P and Seyringer D 2022 *Proc.* (*14th ELEKTRO) (*Krakow, Poland 23-26 May **2022)**

[4] Duan F, Chen K, Chen D and Yu Y. 2021 *Optics Letters* **46** 234-237

[5] Pérez-Armenta C, Ortega-Moñux A, Luque-González J M, Halir R, Reyes-Iglesias P J, Schmid J, Cheben P, Molina-Fernández Í and Wangüemert-Pérez J G 2022 *Photonics Research* **10** A57-65

[6] Soldano L B and Pennings E C 1995 *Journal of lightwave technology.* 1995 **13** 615-627

[7] Zhang L and Xiao J 2021 *JOSA B.* **38** 2830-6

[8] Li Z Z, Han W H and Li Z Y 2020 *Chinese Physics B* **29** 014206

[9] Mahmoud A M, Abdel Aleem S H, Abdelaziz A Y and Ezzat M 2022 *Sustainability* **14** 13299

[10] Maese-Novo A, Halir R, Romero-García S, Pérez-Galacho D, Zavargo-Peche L, Ortega-Moñux A, Molina-Fernández I, Wangüemert-Pérez J G and Cheben P 2013 *Optics express* **21** 7033-7040

[11] Menahem J and Malka D *Materials 15* 5067

[12] Malka D, Sintov Y and Zalevsky Z 2015 *Journal of Optics **17*** 125702

[13] Chen Q, Wang Z, Zhao J, Meng J and He J J 2022 *IEEE Photonics Journal* **14** 1-7

[14] Ogusu, K., 2012 *Japanese Journal of Applied Physics* **51** 082503

[15] Li B, Chua S J, Leitz C W and Fitzgerald E.A 2002 *Optical Engineering* **41** 723-7
[16] Prajzler V, Nekvindova P, Varga M, Kromka A, REMEŠ Z 2014 *J. Optoelectron. Adv. Mater* ***16*** 1226-1231
[17] Leuschner R, Franosch M and Dow T 2008 *Advances in Resist Materials and Processing Technology XXV* **6923** 1131-1138
[18] Hirai Y, Kamei KI, Makino Y, Liu L, Yuan Q, Chen Y and Tabata O 2011 *Procedia Engineering* **25** 1233-6
[19] Mahmoodi A and Tajaddini M 2011 *Proc.* (5th SASTech), (Mashhad, Iran. 12-14 May 2011) pp 1312-420
[20] Lall J and Zappe H 2022. *Smart Materials and Structures* **11** 115014
[21] Dumais P, Wei Y, Li M, Zhao F, Tu X, Jiang J, Celo D, Goodwill D J, Fu H, Geng D and Bernier E 2016 Proc. (OSA Technical Digest) (online **2016**) pp W2A-19
[22] Menahem J and Malka D 2022 *Applied Sciences*, *12* pp 11812
[23] Mohammed Z, Paredes B, Rasras M A 2022 Proc. (OSA Technical Digest) (Online 2022), pp M4J.3